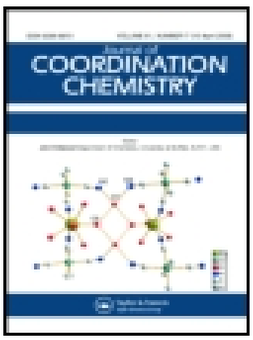

Journal of Coordination Chemistry

ISSN: 0095-8972 (Print) 1029-0389 (Online) Journal homepage: http://www.tandfonline.com/loi/gcoo20

Synthesis and crystal structures of cobalt(III), copper(II), nickel(II) and zinc(II) complexes derived from 4-methoxy-*N*′-(pyridin-2ylmethylene)benzohydrazide with urease inhibitory activity

Guifa Jiang, Huiyuan Yu, Jun-Yan Cheng, Sihan Guo, Wenqi Zhai, Yumin Jiang, Ang Li, Zhiwen Li & Zhonglu You

To cite this article: Guifa Jiang, Huiyuan Yu, Jun-Yan Cheng, Sihan Guo, Wenqi Zhai, Yumin Jiang, Ang Li, Zhiwen Li & Zhonglu You (2018): Synthesis and crystal structures of cobalt(III), copper(II), nickel(II) and zinc(II) complexes derived from 4-methoxy-*N*′-(pyridin-2ylmethylene)benzohydrazide with urease inhibitory activity, Journal of Coordination Chemistry, DOI: 10.1080/00958972.2018.1533959

To link to this article: https://doi.org/10.1080/00958972.2018.1533959

Accepted author version posted online: 08 Oct 2018.

Synthesis and crystal structures of cobalt(III), copper(II), nickel(II) and zinc(II) complexes derived from 4-methoxy-*N′*-(pyridin-2-ylmethylene)benzohydrazide with urease inhibitory activity

GUIFA JIANG†, HUIYUAN YU†, JUN-YAN CHENG‡, SIHAN GUO†, WENQI ZHAI†, YUMIN JIANG†, ANG LI†, ZHIWEN LI† and ZHONGLU YOU*†

†Department of Chemistry and Chemical Engineering, Liaoning Normal University, Dalian 116029, P. R. China
‡College of Chemistry, Chemical Engineering and Material Science, Shandong Normal University, Jinan 250014, P.R. China

Urease catalyzes the decomposition of urea into ammonia, which has harmful effects on both human health and fertile soil. Aiming at exploring novel urease inhibitors, a series of hydrazone compounds and their Co^{III}, Cu^{II}, Ni^{II} and Zn^{II} complexes were prepared from 4-methoxy-*N′*-(pyridin-2-ylmethylene)benzohydrazide (HL). They are [CoClL(NCS)] (**1**), $[CoL_2]\cdot Cl\cdot CH_3OH\cdot H_2O$ (**2**), $[CuL(NCNCN)]_n\cdot nCH_3OH$ (**3**), $[NiL(HL)]\cdot ClO_4\cdot CH_3OH$ (**4**) and $[ZnClL(OH_2)]\cdot CH_3OH$ (**5**). The compounds were characterized by physico-chemical methods. Structures of the complexes were further confirmed by single crystal X-ray diffraction. The metal ions in **1**, **3** and **5** display square pyramidal coordination and **2** and **4** display octahedral coordination. The inhibitory effects of the compounds on *Jack bean* urease were evaluated. The results showed that **3** has effective urease inhibitory activity, with IC_{50} value of (7.3 ± 1.0) $\mu mol\cdot L^{-1}$.

Keywords: Hydrazone; Metal complexes; Crystal structure; Urease inhibition

1. Introduction

Urease (EC 3.5.1.5; urea amidohydrolase) is a binuclear nickel-dependent hydrolase enzyme, which occurs widely in animals and soil [1-3]. Urease enzyme catalyzes the decomposition of urea into ammonia and carbon dioxide in high efficiency [4], with the rate of catalyzed reaction 10^{14} times higher than the non-catalyzed reaction [5]. The enzyme possesses harmful effects on both human health and fertile soil. Bacterial urease is a virulent factor including the formation of infection stones, pyelonephritis, peptic ulceration, hepatic encephalopathy, and other diseases [6-8]. High urease activity in soil leads to increased ammonia toxicity in the air and economic

*Corresponding author. Email: youzhonglu@126.com

problems [9-11]. All these negative effects oblige us to explore effective urease inhibitors. Our research group has pioneered the study of Schiff base and their complexes as urease inhibitors [12-16]. In our previous report, we have identified some copper(II) complexes with Schiff bases or hydrazones as a promising type of lead structures as urease inhibitors [17-20]. Hydrazones have been reported as effective antibacterial agents [21-23] and show interesting urease inhibitory activity [24, 25]. Metal complexes have proved to possess significant inhibitory activities on various enzymes [26, 27]. As part of our ongoing research on urease inhibition with metal complexes, some hydrazones and their Co^{III}, Cu^{II}, Ni^{II} and Zn^{II} complexes are presented here.

2. Experimental

2.1. *Materials and measurements*

2-Pyridinecarboxaldehyde and 4-methoxybenzohydrazide were purchased from Sigma-Aldrich. All other reagents and solvents were purchased from China Chemical Reagent Co. Ltd. *Jack bean* urease was purchased from Sigma-Aldrich. Elemental analyses were performed on a Perkin-Elmer 240C elemental analyzer. IR spectra were recorded on a Jasco FT/IR-4000 spectrometer as KBr pellets from 4000–400 cm^{-1}. UV-Vis spectra were recorded on a Perkin-Elmer Lambda 900 spectrometer. ^{1}H and ^{13}C NMR spectra were recorded on a 500 MHz Bruker Avance instrument. The urease inhibitory activity was measured on a Bio-Tek Synergy HT microplate reader. Single crystal structures were determined using a Bruker D8 Venture single crystal diffractometer.

2.2. *Synthesis of 4-methoxy-N'-(pyridin-2-ylmethylene)benzohydrazide (HL)*

2-Pyridinecarboxaldehyde (0.1 mol, 10.7 g) and 4-methoxybenzohydrazide (0.1 mol, 16.6 g) were mixed in methanol (100 mL). The mixture was stirred for 30 min at room temperature to give a colorless solution. The solution was allowed to stand in air to slowly evaporate to give well-shaped single crystals. The crystals were isolated by filtration, washed three times with cold methanol and dried in air. Yield: 23.2 g (91%). Characteristic IR data (KBr, cm^{-1}): 3189 (NH), 1646 (C=O), 1605 (C=N). UV–Vis data (methanol, λ/nm): 215, 305. Anal. Calcd for $C_{14}H_{13}N_3O_2$: C, 65.9; H, 5.1; N, 16.5. Found: C, 66.1; H, 5.2; N, 16.3%. ^{1}H NMR (500 MHz, DMSO) δ 11.90 (s, 1H, N*H*), 8.62 (d, 1H, Ar*H*), 8.48 (s, 1H, Ar*H*), 7.97-7.86 (m, 4H, Ar*H*), 7.41 (s, 1H, C*H*=N),

7.07 (d, 2H, Ar*H*), 3.84 (s, 3H, CH_3). ^{13}C NMR (126 MHz, DMSO) δ 162.74, 162.14, 153.41, 149.45, 147.38, 136.78, 129.66, 125.21, 124.20, 119.77, 113.74, 55.42.

2.3. ***Synthesis of 1-5***

2.3.1.Chloro-[N-(2-pyridylmethylene)-4-methoxybenzenecarbohydrazonato]-isothiocyanato cobalt(III), [CoClL(NCS)] (1). The Schiff base HL (1.0 mmol, 0.26 g) was dissolved in methanol (20 mL), to which was added dropwise $CoCl_2 \cdot 6H_2O$ (1.0 mmol, 0.24 g) and NH_4NCS (1.0 mmol, 0.076 g) dissolved in methanol (10 mL). The mixture was stirred for 10 min at room temperature and filtered. The filtrate was kept in air for a few days to form crystals suitable for single crystal X-ray diffraction. The crystals were isolated by filtration. Yield: 0.15 g (37%). Characteristic IR data (KBr, cm^{-1}): 2079 (NCS), 1603 (CH=N). UV–Vis data (methanol, λ/nm): 253, 295, 390. Anal. Calcd for $C_{15}H_{12}ClCoN_4O_2S$: C, 44.3; H, 3.0; N, 13.8. Found: C, 44.5; H, 2.9; N, 13.6%. Λ_M (10^{-3} M in acetonitrile): 19 Ω^{-1} cm^2 mol^{-1}.

2.3.2.Bis[N-(2-pyridylmethylene)-4-methoxybenzenecarbohydrazonato]cobalt(III) chloride methanol monohydrate, [CoL$_2$]·Cl·CH$_3$OH·H$_2$O (2). The Schiff base HL (1.0 mmol, 0.26 g) was dissolved in methanol (20 mL), to which was added dropwise $CoCl_2 \cdot 6H_2O$ (1.0 mmol, 0.24 g) dissolved in methanol (10 mL). The mixture was stirred for 10 min at room temperature and filtered. The filtrate was kept in air for a few days to form crystals suitable for single crystal X-ray diffraction. The crystals were isolated by filtration. Yield: 0.17 g (52%). Characteristic IR data (KBr, cm^{-1}): 3345 (OH), 1600 (CH=N). UV–Vis data (methanol, λ/nm): 270, 385. Anal. Calcd for $C_{29}H_{30}ClCoN_6O_6$: C, 53.3; H, 4.6; N, 12.9. Found: C, 53.5; H, 4.6; N, 12.7%. Λ_M (10^{-3} M in acetonitrile): 115 Ω^{-1} cm^2 mol^{-1}.

2.3.3.catena-Poly{[N-(2-pyridylmethylene)-4-methoxybenzenecarbohydrazonato]copper(II) -μ$_{1,5}$-dicyanoamido} methanol, [CuL(NCNCN)]$_n$·nCH$_3$OH (3). The Schiff base HL (1.0 mmol, 0.26 g) was dissolved in methanol (20 mL), to which was added dropwise $CuCl_2 \cdot 2H_2O$ (1.0 mmol, 0.17 g) and $NaN(CN)_2$ (1.0 mmol, 0.089 g) dissolved in methanol (10 mL). The mixture was stirred for 10 min at room temperature and filtered. The filtrate was kept in air for a few days to form crystals suitable for single crystal X-ray diffraction. The crystals were isolated by filtration. Yield: 0.26 g (62%). Characteristic IR data (KBr, cm^{-1}): 3478 (OH), 2309, 2251,

2176 ($N(CN)_2$), 1606 (CH=N). UV–Vis data (methanol, λ/nm): 245, 293, 385. Anal. Calcd for $C_{17}H_{16}CuN_6O_3$: C, 49.1; H, 3.9; N, 20.2. Found: C, 49.1; H, 3.7; N, 20.3%. Λ_M (10^{-3} M in acetonitrile): 16 Ω^{-1} cm^2 mol^{-1}.

2.3.4.[N-(2-pyridylmethylene)-4-methoxybenzenecarbohydrazonato][4-methoxy-N'-(pyridin-2-ylmethylene)benzohydrazido]nickel(II) perchlorate methanol, $[NiL(HL)]\cdot ClO_4\cdot CH_3OH$ (4). The Schiff base HL (1.0 mmol, 0.26 g) was dissolved in methanol (20 mL), to which was added dropwise $Ni(ClO_4)_2\cdot 6H_2O$ (1.0 mmol, 0.37 g) dissolved in methanol (10 mL). The mixture was stirred for 10 min at room temperature and filtered. The filtrate was kept in air for a few days to form crystals suitable for single crystal X-ray diffraction. The crystals were isolated by filtration. Yield: 0.21 g (60%). Characteristic IR data (KBr, cm^{-1}): 3441 (OH), 3263 (NH), 1606 (CH=N), 1101 and 1080 (ClO_4). UV–Vis data (methanol, λ/nm): 310, 350, 375. Anal. Calcd for $C_{29}H_{29}ClN_6NiO_9$: C, 49.8; H, 4.2; N, 12.0. Found: C, 49.7; H, 4.3; N, 11.8%. Λ_M (10^{-3} M in acetonitrile): 130 Ω^{-1} cm^2 mol^{-1}.

2.3.5. Aqua-chlorido-[N-(2-pyridylmethylene)-4-methoxybenzenecarbohydrazonato]zinc(II) methanol, $[ZnClL(OH_2)]\cdot CH_3OH$ (5). The Schiff base HL (1.0 mmol, 0.26 g) was dissolved in methanol (20 mL), to which was added dropwise $ZnCl_2$ (1.0 mmol, 0.136 g) dissolved in methanol (10 mL). The mixture was stirred for 10 min at room temperature and filtered. The filtrate was kept in air for a few days to form crystals suitable for single crystal X-ray diffraction. The crystals were isolated by filtration. Yield: 0.27 g (67%). Characteristic IR data (KBr, cm^{-1}): 3432 (OH), 1605 (CH=N). UV–Vis data (methanol, λ/nm): 278, 320, 373. Anal. Calcd for $C_{15}H_{18}ClN_3O_4Zn$: C, 44.5; H, 4.5; N, 10.4. Found: C, 44.4; H, 4.3; N, 10.3%. Λ_M (10^{-3} M in acetonitrile): 22 Ω^{-1} cm^2 mol^{-1}.

2.4. *X-ray crystallography*

Diffraction intensities for the hydrazones and the complexes were collected at 298(2) K using a Bruker D8 Venture diffractometer with MoKα radiation (λ = 0.71073 Å). The collected data were reduced with SAINT [28], and multi-scan absorption correction was performed using SADABS [29]. Structures of the hydrazones and complexes were solved by direct methods and refined against F^2 by full-matrix least-squares method using SHELXTL [30]. All of the

non-hydrogen atoms were refined anisotropically. The amino and water H atoms in the compounds were located from difference Fourier maps and refined isotropically, with N–H, O–H and H···H distances restrained to 0.90(1), 0.85(1) and 1.37(2) Å, respectively. The remaining hydrogen atoms were placed in calculated positions and constrained to ride on their parent atoms. The thermal parameters for the Cl ion in **1** are larger than other atoms. We have attempted to refine with a disorder model concluding OH, but have not succeeded. The water H atoms of **2** cannot be added accurately because of the disorder of the water molecule. The methanol molecule in **4** is to some extent disordered. Crystallographic data for the hydrazones and the complexes are summarized in table 1. Selected bond lengths and angles are given in table 2.

2.5. *Urease inhibitory activity assay*

The measurement of urease inhibitory activity was carried out according to the literature method [31]. The assay mixture containing 75 μL of *Jack bean* urease and 75 μL of tested compounds with various concentrations (dissolved in DMSO) was pre-incubated for 15 min on a 96-well assay plate. Acetohydroxamic acid was used as a reference. Then 75 μL of phosphate buffer at pH 6.8 containing phenol red (0.18 mmol·L^{-1}) and urea (400 mmol·L^{-1}) were added and incubated at room temperature. The reaction time required for enough ammonium carbonate to form to raise the pH phosphate buffer from 6.8 to 7.7 was measured by a micro-plate reader (560 nm) with end-point being determined by the color change of phenol-red indicator.

3. Results and discussion

3.1. *Chemistry*

The hydrazone compound was readily prepared by the condensation reaction of equimolar quantities of 2-pyridinecarboxaldehyde and 4-methoxybenzohydrazide in methanol (scheme 1). The complexes were prepared by reaction of equimolar quantities of the hydrazone, metal salts, and secondary ligands (NCS for **1**, $N(CN)_2$ for **3**) in methanol. Single crystals of the complexes were obtained by slow evaporation of the methanolic solution of the complexes. Molar conductivities of **1**, **3** and **5** measured in methanol at concentration of 10^{-3} mol·L^{-1} are in the range of 15-50 Ω^{-1} cm^2 mol^{-1}, indicating the non-electrolytic nature of them in such solution [32]. Molar conductivities of **2** and **4** measured in methanol at a concentration of 10^{-3} mol·L^{-1} are in

the range of 100-140 Ω^{-1} cm^2 mol^{-1}, indicating the 1:1 electrolytic nature of them in such solution [32].

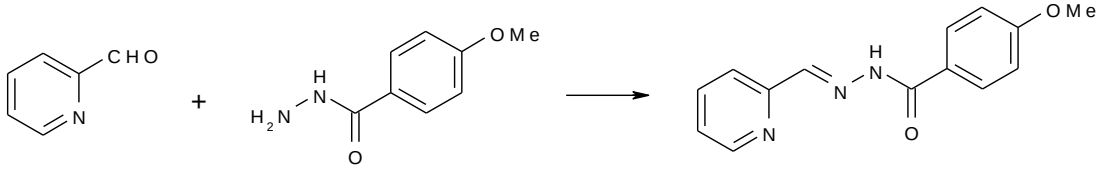

Scheme 1. The synthetic procedure for HL.

3.2. *Structure description of the complexes*

3.2.1. Structure description of 1. The molecular structure of **1** is shown in figure 1. The Co ion is in a square pyramidal geometry, with the pyridine N, imino N, and carbonyl O atoms of the hydrazone ligand, and one thiocyanate N atom located at the basal plane, and with the Cl ligand located at the apical position. The Co ion deviates from the least-squares plane defined by the four basal donor atoms by 0.248(1) Å. The dihedral angle between the pyridine and benzene rings of the hydrazone ligand is 4.6(5)°. The Co-O and Co-N bond lengths are in the range 1.92-2.03 Å, which are comparable to those observed in cobalt(III) complexes with hydrazone ligands [33, 34]. A longer distance is observed for Co-Cl bond length (2.651(5) Å), yet, it is similar to those in other chlorido-coordinated cobalt complexes [35, 36]. In the crystal structure of the complex, the molecules are linked through intermolecular C3–H3···S1 hydrogen bonds [C3–H3 = 0.93 Å, H3···$S1^{i}$ = 2.86 Å, C3···$S1^{i}$ = 3.706(3) Å, C3–H3···$S1^{i}$ = 152(5)°; symmetry code for i: $-x$, $1-y$, $-z$], to form chains along the *c* axis. The chains are further linked *via* weak Cl···N interactions (3.096(3) Å) from the *a* axis to form a two-dimensional network (figure 2). It is not uncommon for the Cl···N interactions. Bathori and coworkers reported a compound bis-2,4-(biphenyl-4-yloxy)-6-chloro-[1,3,5]triazine, in which the Cl···N interactions are 3.05 Å [37].

3.2.2. Structure description of 2. The molecular structure of **2** is shown in figure 3. The compound contains a mononuclear cobalt(III) complex cation, a Cl anion, a methanol and a water molecule of crystallization. The Co ion in the complex is coordinated by two pyridine N, two imino N, and two carbonyl O atoms from two hydrazone ligands, forming an octahedral

geometry. The dihedral angles between the pyridine and benzene rings of the hydrazone ligands are 9.4(4)° and 7.2(4)°. The Co-O and Co-N bond lengths are in the range 1.85-1.93 Å, which are comparable to those observed in cobalt(III) complexes with hydrazone ligands [33, 34]. The Co1-N1 bond in this complex is shorter than that of **1**, which might be caused by the electronic withdrawing effects of the Cl and NCS ligands in **1**. In the crystal structure of the complex, the molecules are linked through O5–H5···Cl1, C15–H15···Cl1^{ii} and C16–H16···Cl1^{iii} hydrogen bonds [O5–H5 = 0.82 Å, H5···Cl1 = 2.37 Å, O5···Cl1 = 3.066(5) Å, O5–H5···Cl1 = 143(5)°; C15–H15 = 0.93 Å, H15···Cl1^{ii} = 2.81 Å, C15···Cl1^{ii} = 3.596(6) Å, C15–H15···Cl1^{ii} = 143(6)°; C16–H16 = 0.93 Å, H16···Cl1^{iii} = 2.74 Å, C16···Cl1^{iii} = 3.619(6) Å, C16–H16···Cl1^{iii} = 157(6)°; symmetry codes for ii: 1/2–*x*, 1/2+*y*, *z*; iii: 1/2+*x*, 1/2–*y*, 1–*z*] to form dimeric structures (figure 4).

3.2.3. Structure description of 3. Molecular structure of **3** is shown in figure 5. The complex is a dicyanoamide bridged polynuclear copper(II) compound. The smallest repeat unit contains a [Cu(NCNCN)L] moiety and a methanol molecule of crystallization. The Cu ion is in a square pyramidal geometry, with the pyridine N, imino N, an enolate O atom of the hydrazone ligand, and one dicyanoamide N atom located at the basal plane, and with another dicyanoamide N atom located at the apical position. The Cu ion deviates from the least-squares plane defined by the four basal donor atoms by 0.300(1) Å. The dihedral angle between the pyridine and benzene rings of the hydrazone ligand is 2.0(5)°. The Cu-O and Cu-N bond lengths in the basal plane are in the range 1.93-2.07 Å, which are comparable to those observed in copper(II) complexes with hydrazone ligands [38, 39]. The Cu1-N6A bond in the apical position of the square pyramid is 2.214(4) Å, indicating it is loosely coordinated to the Cu ion. In the crystal structure of the complex, the methanol molecules are linked to the complex molecules through O3–H3···O1 hydrogen bonds [O3–H3 = 0.82 Å, H3···O1 = 2.26 Å, O3···O1 = 3.034(6) Å, O3–H3···O1 = 159(5)°]. The [CuL] units are linked through dicyanoamide groups to form chains along the *a*-axis (figure 6).

3.2.4. Structure description of 4. The molecular structure of **4** is shown in figure 7. The complex contains a [NiL(HL)]$^{+}$ cation, a perchlorate anion and a methanol molecule of crystallization. The Ni ion is coordinated by two pyridine N, two imino N, one carbonyl O, and

one enolate O atoms, forming an octahedral geometry. The bond Ni1-N2 is longer than that of Ni1-N5, and the bond Ni1-O1 is longer than that of Ni1-O2, which indicates the different types of the hydrazone ligands, one is neutral, and the other one has a negative charge. The dihedral angles between the pyridine and benzene rings of the hydrazone ligands are 7.0(5)° and 19.9(6)°. The Ni-O and Ni-N bond lengths, except Ni1-O1, are in the range 1.96-2.10 Å, which are comparable to those observed in nickel(II) complexes with hydrazone ligands [40, 41]. In the crystal structure of the complex, the perchlorate anions are linked to the complex molecules through C16–H16···O7^{iv} and C18–H18···O6^{v} hydrogen bonds [C16–H16 = 0.93 Å, H16···O7^{iv} = 2.27 Å, C16···O7^{iv} = 3.142(5) Å, C16–H16···O7^{iv} = 155(6)°; C18–H18 = 0.93 Å, H18···O6^{v} = 2.57 Å, C18···O6^{v} = 3.246(6) Å, C18–H18···O6^{v} = 130(6)°; symmetry codes: iv: –*x*, 1–*y*, 1–*z*; v: iv: *x*, –1+*y*, 1+*z*]. The methanol molecules are linked to the complex molecules through O9–H9A···N6^{vi} and C27–H27···O9^{vii} hydrogen bonds [O9–H9A = 0.82 Å, H9A···N6^{vi} = 2.06 Å, O9···N6^{vi} = 2.855(5) Å, O9–H9A···N6^{vi} = 164(5)°; C27–H27 = 0.93 Å, H27···O9^{vii} = 2.56 Å, C27···O9^{vii} = 3.474(6) Å, C27–H27···O9^{vii} = 168(7)°; symmetry codes: vi: 1+*x*, *y*, *z*; vii: –1+*x*, *y*, *z*]. Adjacent complex molecules are linked through N3–H3···O2^{viii} hydrogen bonds [N3–H3 = 0.90 Å, H3···O2^{viii} = 1.87 Å, N3···O2^{viii} = 2.729(5) Å, N3–H3···O2^{viii} = 159(6)°; symmetry code for viii: 1–*x*, 1–*y*, 1–*z*] to form dimers. The dimers are further linked through C12–H12···O4^{ix} hydrogen bonds [C12–H12 = 0.93 Å, H12···O9^{ix} = 2.57 Å, C12···O9^{ix} = 3.474(6) Å, C12–H12···O9^{ix} = 165(7)°; symmetry code for ix: *x*, *y*, 1+*z*] to form chains along the *c*-axis (figure 8).

3.2.5. Structure description of 5. The molecular structure of **5** is shown in figure 9. The complex contains a [ZnClL(OH_2)] complex molecule and a methanol molecule of crystallization. The Zn ion is in a square pyramidal geometry, with the pyridine N, imino N, and enolate O atom of the hydrazone ligand, and one Cl ligand located in the basal plane, and with one water O atom located at the apical position. The Zn ion deviates from the least-squares plane defined by the four basal donor atoms by 0.432(1) Å. The dihedral angle between the pyridine and benzene rings of the hydrazone ligand is 10.5(3)°. The Zn-O and Zn-N bond lengths are in the range 2.01-2.09 Å, which are comparable to those observed in zinc(II) complexes with hydrazone ligands [42]. A longer distance is observed for Zn-Cl bond length (2.2559(9) Å), yet, it is similar to those in chlorido-coordinated zinc complexes [43, 44]. In the crystal structure of the complex, adjacent complex molecules are linked through O3–H3A···N3^{viii} hydrogen bonds [O3–H3A =

0.84 Å, H3A···N3^{viii} = 1.91 Å, O3···N3^{viii} = 2.756(5) Å, O3–H3A···N3^{viii} = 175(5)°] to form dimers. The dimers are further linked by methanol and water molecules through O4–H4···Cl1^{vii} and O3–H3B···O4 hydrogen bonds [O4–H4 = 0.82 Å, H4···Cl1^{vii} = 2.39 Å, O4···Cl1^{vii} = 3.208(5) Å, O4–H4···Cl1^{vii} = 173(6)°; O3–H3B = 0.84 Å, H3B···O4 = 1.87 Å, O3···O4 = 2.709(5) Å, O3–H3B···O4 = 178(6)°] to form chains along the *a*-axis (figure 10).

3.3. *IR and UV-Vis spectra*

The medium and broad absorptions in the region 3300–3500 cm^{-1} in the spectra of **2-5** substantiate the presence of O–H groups. The sharp bands indicative of the N–H vibrations of HL and **4** are located at 3189 and 3263 cm^{-1}, respectively. The intense band indicative of the C=O vibration of HL is observed at 1646 cm^{-1}, however, it is absent in the spectra of the complexes, indicating the enolisation of the amide functionality and subsequent proton replacement by the metal ions. The strong absorption bands in the region 1600–1610 cm^{-1} for HL and the complexes are assigned to the azomethine ν(C=N) [45]. The typical absorptions at 2079 cm^{-1} for **1** is assigned to the vibration of the NCS ligand, at 2176 cm^{-1} for **3** is assigned to the vibration of the $N(CN)_2$ ligand, and at 1080 cm^{-1} for **4** is assigned to the vibration of the perchlorate anion.

Electronic spectra of the complexes were recorded at 10^{-5} M in methanol. The complexes displayed strong bands centered at 290-320 nm, which can be assigned to the n–π* transition of the chromophore (-C=N-NH-CO). The charge transfer LMCT bands are located in the range 370–400 nm.

3.4. *Pharmacology study*

The inhibition curves of the complexes are shown in scheme 2. The percent inhibition of the complexes on *Jack bean* urease are summarized in table 3. Complex **3** shows effective urease inhibitory activity, with IC_{50} value of (7.3 ± 1.0) μmol·L^{-1}. The remaining complexes have no or weak activity. As a comparison, acetohydroxamic acid (AHA) was used as a reference drug with the percent inhibition of (84.3 ± 3.9)% and with IC_{50} value of (37.2 ± 4.0) μmol·L^{-1}. Copper perchlorate can inhibit urease activity, with IC_{50} value of (8.8 ± 1.4) μmol·L^{-1}. Cobalt perchlorate, nickel perchlorate and zinc perchlorate have weak or no activity against the urease. The copper complex **3** has stronger activities than the copper(II) complex with *N*-hydroxyethyl-*N*-

benzimidazolylmethylethylenediaminediacetic acid (IC_{50} = 35 μM) [46], and also better than the copper(II) complexes with Schiff base ligands (IC_{50} = 19 and 39 μM) [47], and comparable to those with hydrazone ligands (IC_{50} = 1.5-18.3 μmol·L^{-1}) [48].

The coordination geometries of the metals and the secondary ligands may influence the inhibition potential of the complexes. For **1** and **5**, there are Cl ligands, which are difficult to substitute by the thiol group of the active center of the urease. For **2** and **4**, the metals are in octahedral coordination, which are in a sealed cavity, and difficult to interact with the enzyme. For **3**, the dicyanoamide ligand is loosely coordinated in the apical position of the square pyramidal geometry, which can be readily substituted by the thiol group of the enzyme, and block the entrance of the active pocket.

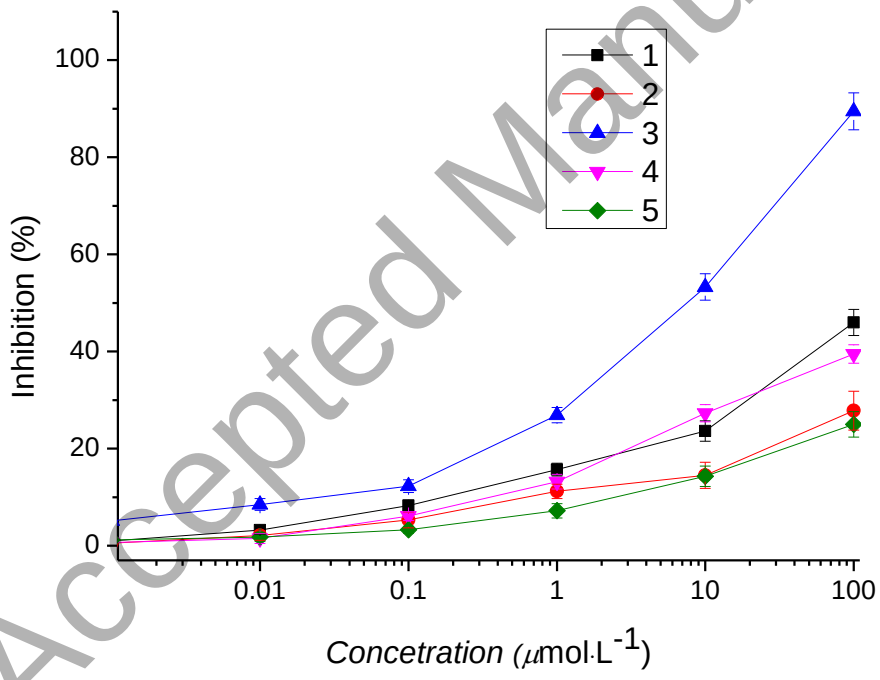

Scheme 2. Inhibition curves of the complexes.

4. Conclusion

The present study reports the syntheses, characterization and crystal structures of new complexes of Co^{III}, Cu^{II}, Ni^{II} and Zn^{II}. The copper complex has effective urease inhibitory activity, which can be further optimized and developed as prospective lead urease inhibitor.

Supplementary data

CCDC 1812960 (**1**), 1812961 (**2**), 1813292 (**3**), 1812962 (**4**) and 1812963 (**5**) contain the supplementary crystallographic data for this paper. These data can be obtained free of charge *via* http://www.ccdc.cam.ac.uk/conts/retrieving.html, or from the Cambridge Crystallographic Data Centre, 12 Union Road, Cambridge CB2 1EZ, UK; Fax: (+44) 1223-336-033; or E-mail: deposit@ccdc.cam.ac.uk.

Disclosure statement

No potential conflict of interest was reported by the authors.

Funding

This work was financially supported by the Natural Science Foundation of China (Project No. 21641012), the Innovative Entrepreneurial Training Program of Liaoning Normal University (Project No. cx201802017), and the Education Office of Liaoning Province (Project No. LF201783611).

References

[1] T. Myrach, A.T. Zhu, C.P. Witte. *J. Biol. Chem.*, **292**, 14556 (2017).

[2] T. Arshad, K.M. Khan, N. Rasool, U. Salar, S. Hussain, H. Asghar, M. Ashraf, A. Wadood, M. Riaz, S. Perveen. *Bioorg. Chem.*, **72**, 21 (2017).

[3] S. Yalcin, A. Basman. *Food Chem.*, **169**, 203 (2015).

[4] A.B. Mira, H. Cantarella, G.J.M. Souza-Netto, L.A. Moreira, M.Y. Kamogawa, R. Otto. *Agr. Ecosyst. Environ.*, **248**, 105 (2017).

[5] R.J. Dempsey, N.A. Slaton, R.J. Norman, T.L. Roberts. *Agron. J.*, **109**, 363 (2017).

[6] M. Taha, N.H. Ismail, S. Imran, A. Wadood, F. Rahim, M. Riaz. *J. Bioorg. Med. Chem.*, **23**, 7211 (2015).

[7] A. Hameed, K.M. Khan, S.T. Zehra, R. Ahmed, Z. Shafiq, S.M. Bakht, M. Yaqub, M. Hussain, A.D.L.V.D. Leon, F.N.J. Bajorath, H. Ahmad, M.N. Tahir, M.I. Choudhary. *J. ACS. Med. Chem. Lett.*, **1**, 145 (2010).

[8] Z. Amtul, R.A. Siddiqui, M.I. Choudhary. *Curr. Med. Chem.*, **9**, 1323 (2002).

[9] M.A.S. Aslam, S.U. Mahmood, M. Shahid, A. Saeed, J. Iqbal. *Eur. J. Med. Chem.*, **46**, 5473 (2011).

[10] A. Saeed, S. Zaib, A. Pervez, A. Mumtaz, M. Shahid, J. Iqbal. *Med. Chem. Res.*, **22**, 3653 (2013).

[11] A. Saeed, M.S. Khan, H. Rafique. *Bioorg. Chem.*, **52**, 1 (2014).

[12] C.L. Jing, C.F. Wang, K. Yan, K.D. Zhao, G.H. Sheng, D. Qu, F. Niu, H.L. Zhu, Z.L. You. *Bioorg. Med. Chem.*, **24**, 270 (2016).

[13] Y.Y. Zhu, C.F. Wang, K. Yan, K.D. Zhao, G.H. Sheng, Q.Q.G. Hu, L.Y. Zhang, Z.L. You. *J. Coord. Chem.*, **69**, 2493 (2016).

[14] Z.L. You, M.Y. Liu, C.F. Wang, G.H. Sheng, X.L. Zhao, D. Qu, F. Niu. *RSC Adv.*, **6**, 16679 (2016).

[15] D. Qu, F. Niu, X.L. Zhao, K.X. Yan, Y.T. Ye, J. Wang, M. Zhang, Z.L. You. *Bioorg. Med. Chem.*, **23**, 1944 (2015).

[16] X.F. Chen, C.F. Wang, S. Kong, C. Li, X. Zhou, C.Y. Zhang, G.H. Sheng, H.L. Zhu. *J. Struct. Chem.*, **58**, 797 (2017).

[17] Z.L. You, H.Y. Yu, B.Y. Zheng, C.L. Zhang, C.W. Lv, K. Li, L. Pan. *Inorg. Chim. Acta*, **469**, 44 (2018).

[18] S.H. Guo, T.R. Wang, J.J. Xin, Q.Q.G. Hu, S.F. Ren, G.H. Sheng, L. Pan, C.L. Zhang, K. Li, Z.L. You. *J. Coord. Chem.*, **70**, 3449 (2017).

[19] J. Wang, D. Qu, J.X. Lei, Z.L. You. *J. Coord. Chem.*, **70**, 544 (2017).

[20] L. Pan, C.F. Wang, K. Yan, K.D. Zhao, G.H. Sheng, H.L. Zhu, X.L. Zhao, D. Qu, F. Niu, Z.L. You. *J. Inorg. Biochem.*, **159**, 22 (2016).

[21] G.C. Wang, M. Chen, J. Wang, Y.P. Peng, L.Y. Li, Z.Z. Xie, B. Deng, S. Chen, W.B. Li. *Bioorg. Med. Chem. Lett.*, **27**, 2957 (2017).

[22] M.A. Abdelrahman, I. Salama, M.S. Gomaa, M.M. Elaasser, M.M. Abdel-Aziz, D.H. Soliman. *Eur. J. Med. Chem.*, **138**, 698 (2017).

[23] V. Gorantla, R. Gundla, S.S. Jadav, S.R. Anugu, J. Chimakurthy, S.K. Nidasanametla, R. Korupolu. *New J. Chem.*, **41**, 13516 (2017).

[24] M. Taha, N.H. Ismail, M.S. Baharudin, S. Lalani, S. Mehboob, K.M. Khan, S. Yousuf, S. Siddiqui, F. Rahim, M.I. Choudhary. *Med. Chem. Res.*, **24**, 1325 (2015).

[25] K.M. Khan, F. Rahim, A. Khan, S. Ali, M. Taha, S.M. Saad, M. Khan, Najeebullah, A. Shaikh, S. Perveen. *J. Chem. Soc. Pakistan*, **37**, 479 (2015).

[26] Q.P. Qin, T. Meng, M.X. Tan, Y.C. Liu, X.J. Luo, B.Q. Zou, H. Liang. *Eur. J. Med. Chem.*, **143**, 1597 (2018).

[27] V. Oliveri, V. Lanza, D. Milardi, M. Viale, I. Maric, C. Sgarlata, G. Vecchio. *Metallomics*, **9**, 1439 (2017).

[28] Bruker, SMART (Version 5.628) and SAINT (Version 6.02); Bruker AXS: Madison, Wisconsin, USA (1998).

[29] G.M. Sheldrick, SADABS Program for Empirical Absorption Correction of Area Detector, University of Göttingen: Germany (1996).

[30] G.M. Sheldrick. *Acta Crystallogr.*, **A64**, 112 (2008).

[31] W.-J. Mao, P.-C. Lv, L. Shi, H.-Q. Li, H.-L. Zhu. *Bioorg. Med. Chem.*, **17**, 7531 (2009).

[32] W.J. Geary. *Coord. Chem. Rev.*, **7**, 81 (1971).

[33] C.V. Garcia, G.L. Parrilha, B.L. Rodrigues, P.J.S. Barbeira, R.M. Clarke, T. Storr, H. Beraldo. *Polyhedron*, **124**, 86 (2017).

[34] G. Mahmoudi, H. Chowdhury, S.E. Lofland, B.K. Ghosh, A.M. Kirillov. *J. Coord. Chem.*, **70**, 1973 (2017).

[35] M. Fleck, M. Layek, R. Saha, D. Bandyopadhyay. *Transition Met. Chem.*, **38**, 715 (2013).

[36] J. Welby, L.N. Rusere, J.M. Tanski, L.A. Tyler. *Inorg. Chim. Acta*, **362**, 1405 (2009).

[37] N. Bathori, L. Bihatsi, P. Bombicz, M. Czugler. *CrystEngComm*, **5**, 42 (2003).

[38] K. Hu, G.M. Zhou, Z. Zhang, F.Y. Li, J.G. Li, F.P. Liang. *RSC Adv.*, **6**, 36077 (2016).

[39] K. Roztocki, D. Matoga, W. Nitek. *Inorg. Chim. Acta*, **448**, 86 (2016).

[40] U. Kendur, G.H. Chimmalagi, S.M. Patil, K.B. Gudasi, C.S. Frampton, C.V. Mangannavar, I.S. Muchchandi. *J. Mol. Struct.*, **1153**, 299 (2018).

[41] F.A. Afkhami, A.A. Khandar, G. Mahmoudi, M. Amini, E. Molins, P. Garczarek, J. Lipkowski, J.M. White, A.M. Kirillov. *Inorg. Chim. Acta*, **458**, 68 (2017).

[42] L. Li, Y.Z. Zhang, E. Liu, C.X. Yang, J.A. Golen, A.L. Rheingold, G.Q. Zhang. *J. Mol. Struct.*, **1110**, 180 (2016).

[43] N. Filipovic, M. Borna, O. Klisuric, M. Pregelj, M. Jagodic, K. Andelkovic, T. Todorovic. *J. Coord. Chem.*, **66**, 1549 (2013).

[44] P.U. Maheswari, S. Barends, S. Ozalp-Yaman, P. de Hoog, H. Casellas, S.J. Teat, C. Massera, M. Lutz, A.L. Spek, G.P. van Wezel, P. Gamez, J. Reedijk. *Chem. Eur. J.*, **13**, 5213 (2007).

[45] R.A. Lal, S. Choudhury, A. Ahmed, M. Chakraborty, R. Borthakur, A. Kumar. *J. Coord. Chem.*, **62**, 3864 (2009).

[46] L. Habala, A. Roller, M. Matuska, J. Valentova, A. Rompel, F. Devinsky. *Inorg. Chim. Acta*, **421**, 423 (2014).

[47] Y. Gou, M. Yu, Y. Li, Y. Peng, W. Chen. *Inorg. Chim. Acta*, **404**, 224 (2013).

[48] F. Niu, K.-X. Yan, L. Pang, D. Qu, X. Zhao, Z. You. *Inorg. Chim. Acta*, **435**, 299 (2015).

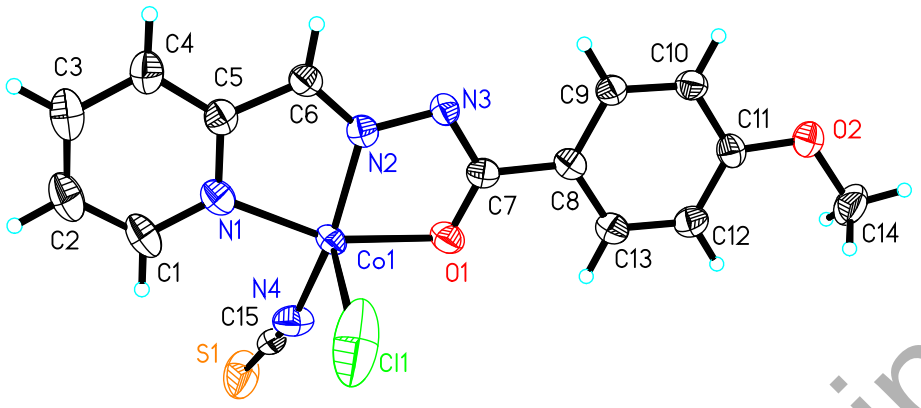

Figure 1. Molecular structure of **1** showing the atom-numbering scheme. Displacement ellipsoids are drawn at 30% probability level.

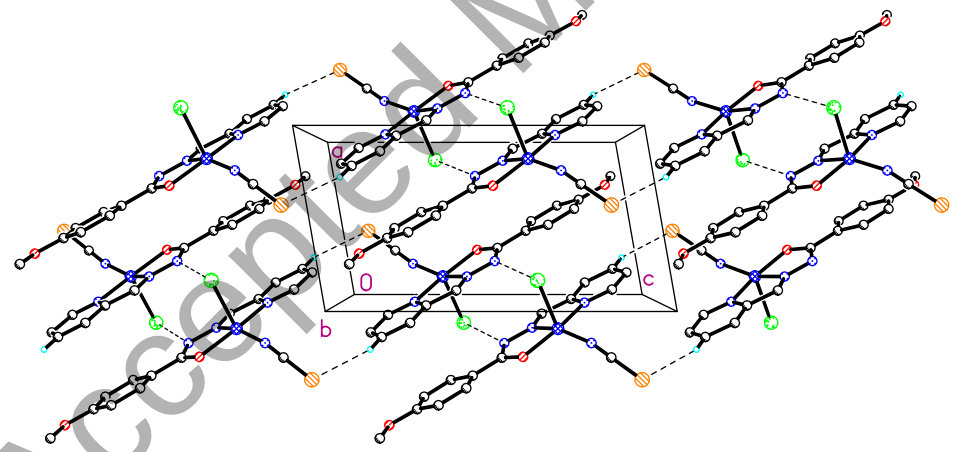

Figure 2. Molecular packing structure of **1** viewed along the *b* axis. Hydrogen bonds shown as dashed lines.

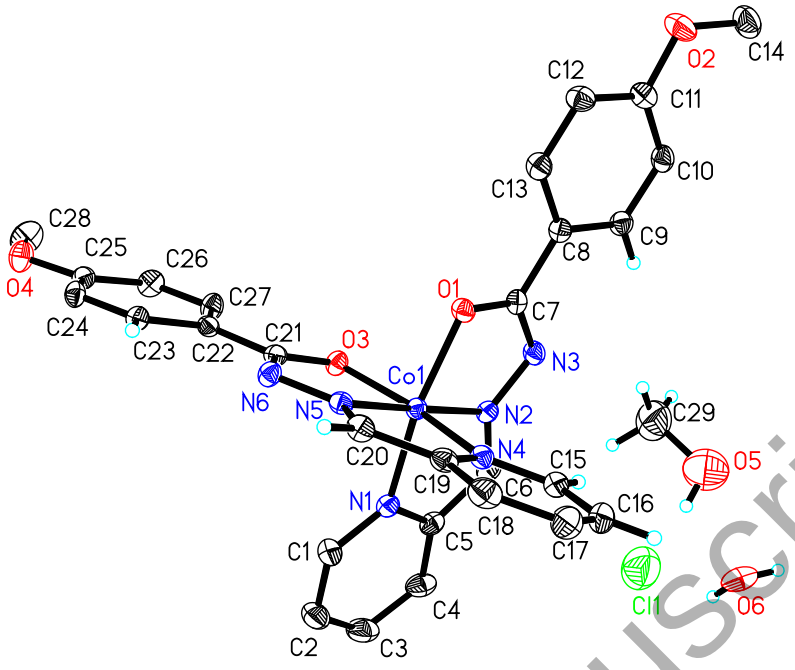

Figure 3. Molecular structure of **2** showing the atom-numbering scheme. Displacement ellipsoids are drawn at 30% probability level.

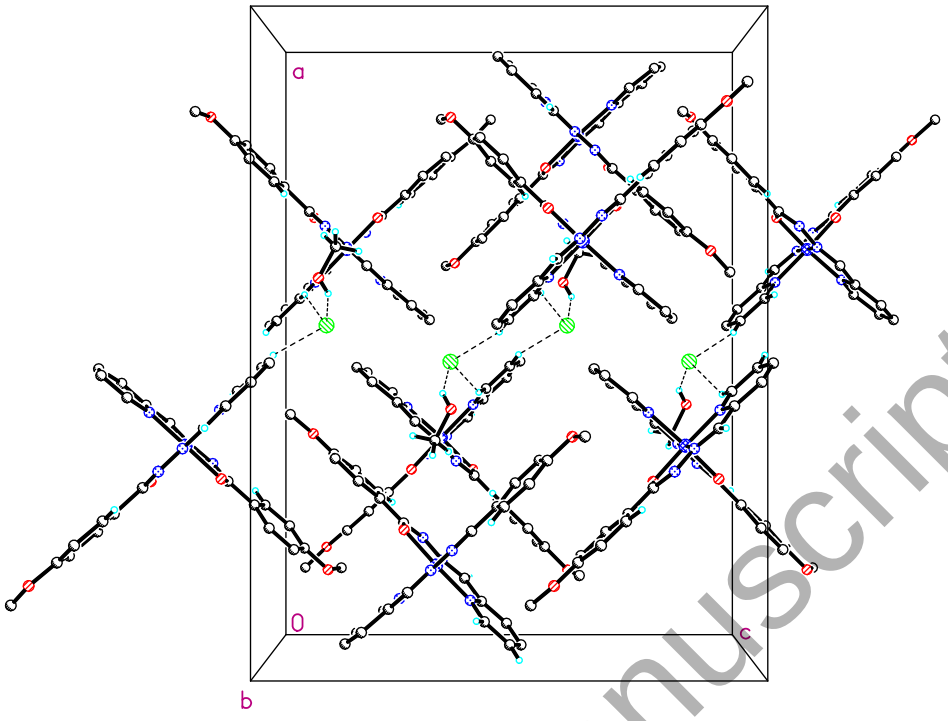

Figure 4. Molecular packing structure of **2** viewed along the *b* axis. Hydrogen bonds shown as dashed lines.

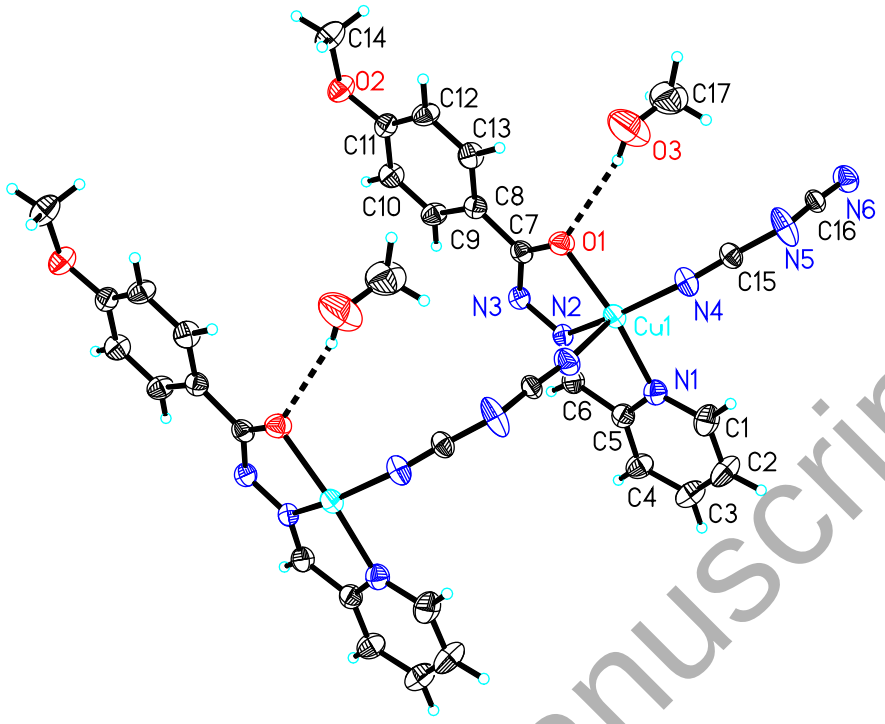

Figure 5. Molecular structure of **3** showing the atom-numbering scheme. Displacement ellipsoids are drawn at 30% probability level.

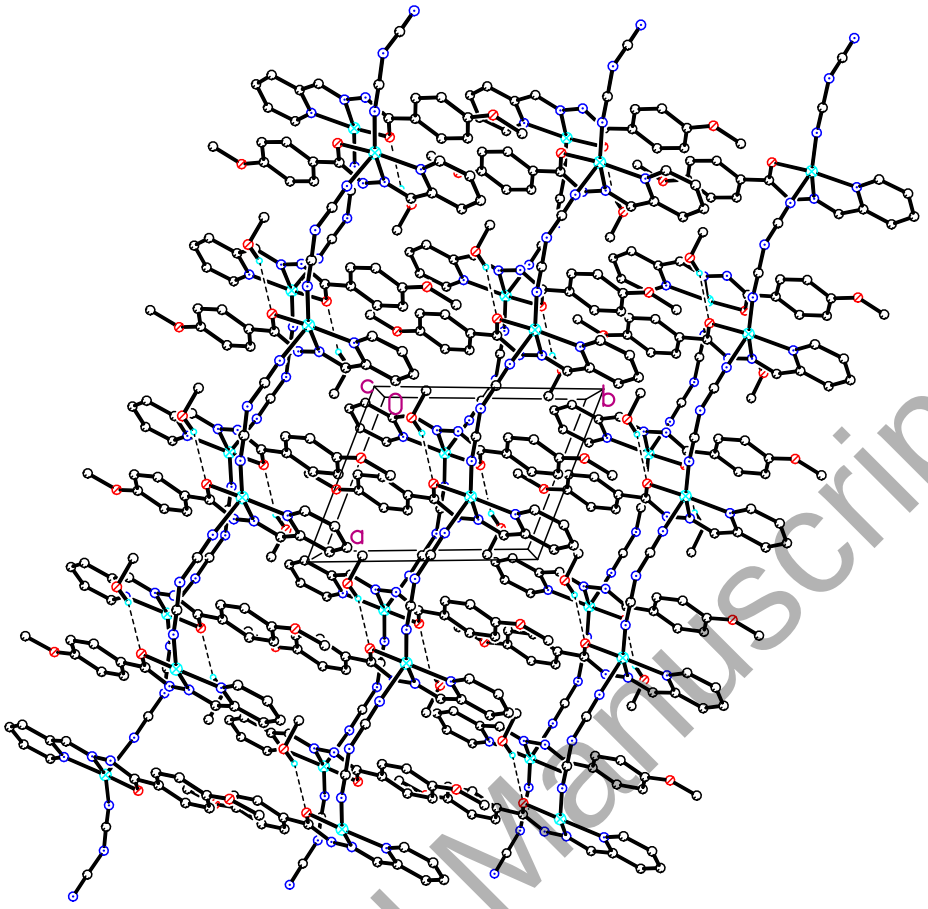

Figure 6. Molecular packing structure of **3** viewed along the *c* axis. Hydrogen bonds shown as dashed lines.

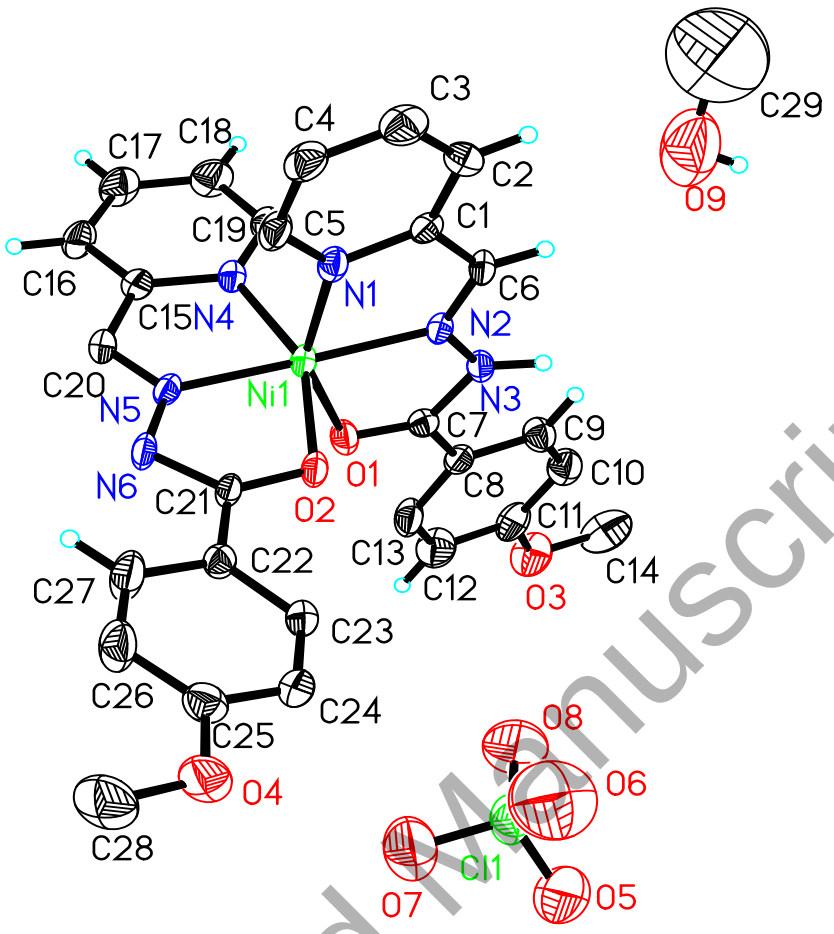

Figure 7. Molecular structure of **4** showing the atom-numbering scheme. Displacement ellipsoids are drawn at 30% probability level.

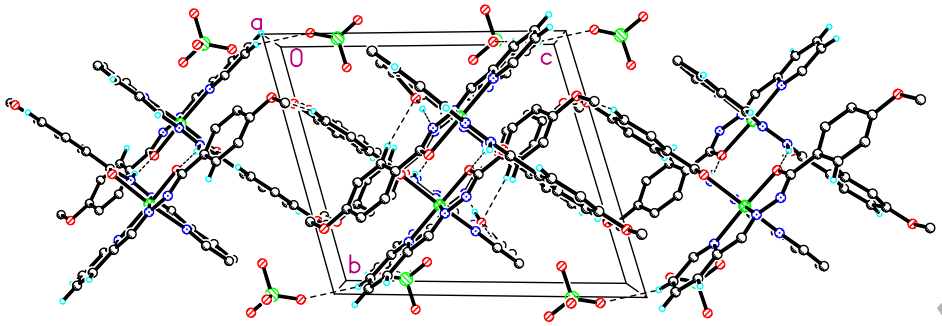

Figure 8. Molecular packing structure of **4** viewed along the *b* axis. Hydrogen bonds shown as dashed lines.

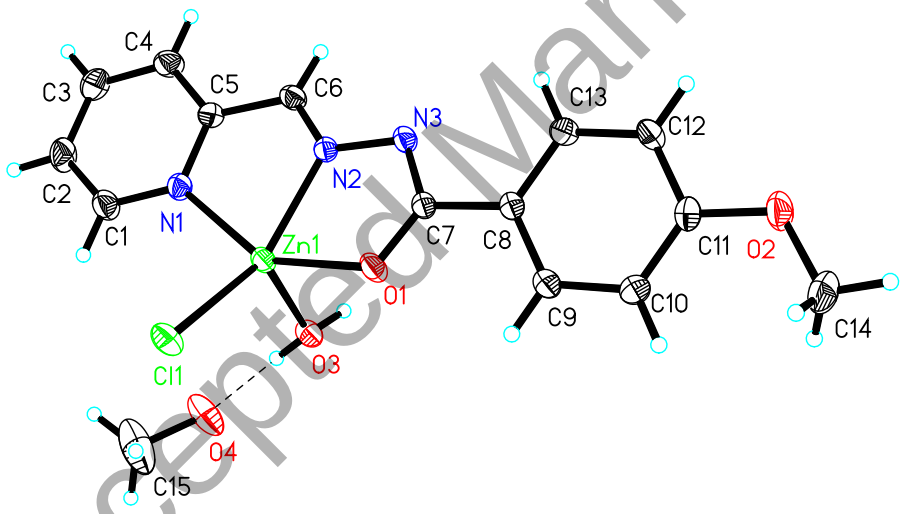

Figure 9. Molecular structure of **5** showing the atom-numbering scheme. Displacement ellipsoids are drawn at 30% probability level.

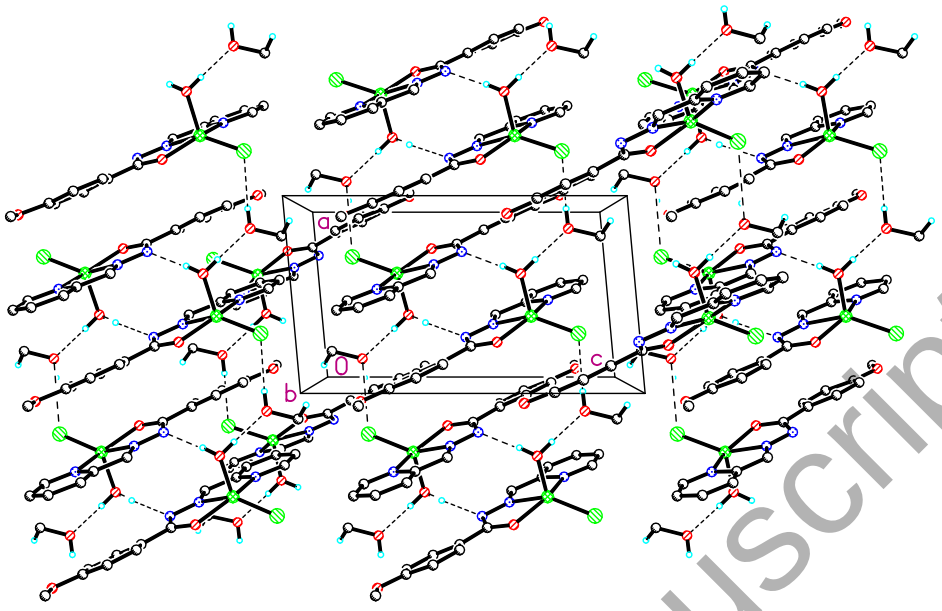

Figure 10. Molecular packing structure of **5** viewed along the *b* axis. Hydrogen bonds shown as dashed lines.

Table 1. Crystal data for **1**-**5**.

	1	**2**	**3**	**4**	**5**
Formula	$C_{15}H_{12}ClCoN_4O_2S$	$C_{29}H_{30}ClCoN_6O_6$	$C_{17}H_{16}CuN_6O_3$	$C_{29}H_{29}ClN_6NiO_9$	$C_{15}H_{18}ClN_3O_4Zn$
FW	406.73	652.97	415.90	699.74	405.14
Crystal shape / color	Block / brown	Block / brown	Block / blue	Block / brown	Block / colorless
Crystal size/mm	0.19×0.18×0.15	0.30×0.27×0.26	0.25×0.23×0.22	0.21×0.18×0.17	0.35×0.32×0.30
Crystal system	Monoclinic	Orthorhombic	Triclinic	Triclinic	Monoclinic
Space group	$P2_1/n$	*Pbcn*	*P*-1	*P*–1	$P2_1/c$
a (Å)	7.384(2)	25.314(2)	7.543(2)	10.885(2)	7.546(1)
b (Å)	17.681(2)	12.187(2)	9.857(2)	11.718(1)	17.454(2)
c (Å)	13.715(2)	19.422(2)	13.840(1)	13.196(2)	13.076(2)
α (°)	90	90	108.260(2)	72.325(2)	90
β (°)	99.941(2)	90	91.090(2)	79.037(2)	95.197(2)
γ (°)	90	90	109.648(2)	79.733(2)	90
V (Å^3)	1763.7(5)	5991.9(12)	911.5(3)	1561.3(4)	1715.2(4)
Z	4	8	2	2	4
λ (MoKα) (Å)	0.71073	0.71073	0.71073	0.71073	0.71073
T (K)	298(2)	298(2)	298(2)	298(2)	298(2)
μ (Mo*K*α) (cm^{-1})	1.257	0.715	1.229	0.770	1.612
T_{min}	0.7961	0.8142	0.7487	0.8550	0.6024
T_{max}	0.8338	0.8360	0.7738	0.8803	0.6435
Reflections / parameters	9433 / 218	33859 / 398	4752 / 247	8323 / 459	9818 / 226
Unique reflections	3209	5590	3328	5690	3176
Observed reflections [$I > 2\sigma(I)$]	2068	4397	2280	2966	2523
Restraints	0	3	0	120	3
Goodness of fit on F^2	1.072	1.081	1.042	0.989	1.052
R_1, wR_2 [$I > 2\sigma(I)$]	0.0726, 0.1424	0.0668, 0.2244	0.0573, 0.1353	0.0760, 0.1749	0.0404, 0.0805
R_1, wR_2 (all data)	0.1225, 0.1661	0.0834, 0.2465	0.0935, 0.1586	0.1546, 0.2239	0.0570, 0.0887

Table 2. Selected bond lengths (Å) and angles (°) for **1**-**5**.

	1	**2**	**3**	**4**	**5**
	M = Co	M = Co	M = Cu	M = Ni	M = Zn
M1–N1	2.030(6)	1.928(4)	2.068(4)	2.093(6)	2.185(2)
M1–N2	1.926(5)	1.853(4)	1.934(4)	2.001(5)	2.070(2)
M1–O1	1.990(4)	1.911(3)	2.011(3)	2.182(5)	2.090(2)
Co1–N4	1.962(7)	1.928(4)			
Co1–Cl1	2.637(4)				
Co1–N5		1.858(4)			
Co1–O3		1.910(3)			
Cu1–N4			1.970(4)		
Cu1–N6A			2.214(4)		
Ni1–N5				1.967(5)	
Ni1–O2				2.089(5)	
Ni1–N4				2.094(5)	
Zn1–O3					2.010(2)
Zn1–Cl1					2.2559(9)
N2–M1–N1	80.0(2)	83.23(16)	80.28(16)	78.0(2)	75.75(9)
O1–M1–N1	158.7(2)	164.67(15)	157.84(15)	152.36(19)	149.20(9)
N2–M1–O1	79.0(2)	81.55(14)	78.85(15)	74.32(19)	74.37(9)
N2–Co1–N4	158.8(2)	96.38(15)			
N4–Co1–O1	100.1(2)	91.15(15)			
N4–Co1–N1	98.0(3)	92.29(16)			
N2–Co1–Cl1	104.15(17)				
N4–Co1–Cl1	97.1(2)				
O1–Co1–Cl1	93.44(16)				
N1–Co1–Cl1	95.37(17)				
N2–Co1–N5		178.56(16)			
N5–Co1–O3		81.32(14)			
N2–Co1–O3		98.66(14)			
N5–Co1–O1		97.01(14)			
O3–Co1–O1		90.91(13)			
N5–Co1–N1		98.21(15)			
O3–Co1–N1		89.63(15)			
N5–Co1–N4		83.65(15)			
O3–Co1–N4		164.96(14)			
N2–Cu1–N4			158.80(17)		
N4–Cu1–O1			99.87(16)		
N4–Cu1–N1			96.87(17)		
N2–Cu1–N6A			101.57(16)		
O1–Cu1–N6A			96.02(15)		
N4–Cu1–N6A			99.61(17)		
N1–Cu1–N6A			95.38(16)		
N5–Ni1–N2				177.6(2)	

N5–Ni1–O2	75.87(19)	
N2–Ni1–O2	103.99(18)	
N5–Ni1–N1	99.6(2)	
O2–Ni1–N1	92.13(19)	
N5–Ni1–N4	79.2(2)	
N2–Ni1–N4	101.1(2)	
O2–Ni1–N4	154.67(19)	
N1–Ni1–N4	96.4(2)	
N5–Ni1–O1	108.08(19)	
O2–Ni1–O1	94.18(18)	
N4–Ni1–O1	89.20(19)	
O3–Zn1–N2		104.38(10)
O3–Zn1–O1		93.31(10)
O3–Zn1–N1		101.15(10)
O3–Zn1–Cl1		106.33(7)
O1–Zn1–Cl1		101.69(7)
N2–Zn1–Cl1		149.21(8)
N1–Zn1–Cl1		100.10(7)

Table 3. Inhibition of urease by the tested materials.

Tested materials	Percentage inhibition rate[#]	IC_{50} (μmol·L^{-1})
1	46.0 ± 2.7	> 100
2	27.8 ± 4.0	> 100
3	89.5 ± 3.8	7.3 ± 1.0
4	39.5 ± 1.9	> 100
5	25.0 ± 2.6	> 100
HL	–	> 100
Copper perchlorate	87.5 ± 2.6	8.8 ± 1.4
Cobalt perchlorate	35.5 ± 2.1	> 100
Nickel perchlorate	22.9 ± 3.3	> 100
Zinc perchlorate	–	> 100
Acetohydroxamic acid	84.3 ± 3.9	37.2 ± 4.0

[#] The concentration of the tested material is 100 μmol·L^{-1}. – indicates no activity.

Graphical abstract